Type III ω-Agatoxins: A Family of Probes for Similar Binding Sites on L- and N-Type Calcium Channels

Eric A. Ertel,‡ Vivien A. Warren,‡ Michael E. Adams,§ Patrick R. Griffin,∥ Charles J. Cohen,‡ and McHardy M. Smith*,‡

Department of Membrane Biochemistry and Biophysics and Department of Analytical Biochemistry, Merck Research Laboratories, Rahway, New Jersey 07065, and Departments of Entomology and Neuroscience, University of California, Riverside, California 92521

Received November 30, 1993; Revised Manuscript Received February 10, 1994®

ABSTRACT: The peptide ω-agatoxin-IIIA (ω-Aga-IIIA) from venom of the funnel web spider *Agelenopsis aperta* is the only known agent that blocks L-type and N-type Ca channels with equal high potency (IC_{50} ≤ 1 nM). From the same venom, we have purified and sequenced a family of peptides which are homologous to ω-Aga-IIIA but vary over 100-fold in their relative affinity for L-type versus N-type Ca channels. One of these, ω-Aga-IIIB, is 76 amino acids long and identical to ω-Aga-IIIA in 66 positions. We identified two other similar peptides, ω-Aga-IIIC and ω-Aga-IIID, as well as one single amino acid variant of ω-Aga-IIIA and two of ω-Aga-IIIB. The type III ω-agatoxins exhibit similar but distinct activities on voltage-gated Ca channels. ω-Aga-IIIA, ω-Aga-IIIB, and ω-Aga-IIID are nearly indistinguishable in their actions at the insect neuromuscular junction (no effect at 0.1 μM), on atrial T-type Ca channels (no effect at 0.5 μM), and in two assays for synaptosomal Ca channels: they are nearly equipotent inhibitors of ^{125}I-ω-conotoxin GVIA binding to rat brain synaptic membranes (IC_{50} = 0.17–0.33 nM) and blockers of the K^+-induced $^{45}Ca^{2+}$ influx into chick brain synaptosomes (ω-Aga-IIIB, 1.2 nM; ω-Aga-IIIA, 2.4 nM). In contrast, ω-Aga-IIIA is a better blocker of locust Ca channels (IC_{50} ≈ 10–50 nM) than is ω-Aga-IIIB. Finally, although ω-Aga-IIIA, ω-Aga-IIIB, and ω-Aga-IIID all block atrial L-type Ca channels, ω-Aga-IIIA is over 100-fold more potent. Thus, although type III ω-agatoxins appear to recognize a binding site common to L- and N-type Ca channels, ω-Aga-IIIB and ω-Aga-IIID identify differences between the two channels.

Peptide toxins are valuable tools for the characterization of ion channels. The venom of the funnel web spider *Agelenopsis aperta* contains the ω-agatoxins, an assortment of peptides that block voltage-gated Ca channels (Adams et al., 1990; Mintz et al., 1992b; Venema et al., 1992). Two of these, ω-agatoxin-IIIA (ω-Aga-IIIA)[1] and ω-agatoxin-IVA (ω-Aga-IVA), are used extensively to classify vertebrate Ca channels (Mintz et al., 1991, 1992a,b; Cohen et al., 1992a; Pocock et al., 1992; Turner et al., 1992, 1993; Ertel et al., 1994; Sather et al., 1993; Soong et al., 1993). Vertebrate voltage-gated Ca channels have been classified according to biophysical and pharmacological properties (Tsien et al., 1991; Snutch & Reiner, 1992). They have been divided into two broad categories of "low voltage activated" (or T-type) and "high voltage activated" channels, based upon differences in the time and voltage dependences of channel gating. The high voltage activated channels have been further classified into three subtypes (L-, N-, and P-type) based upon pharmacological properties. L-type Ca channels are defined as being sensitive to 1,4-dihydropyridines (DHPs), especially the DHP "agonists", whereas N-type and P-type Ca channels are defined as being blocked by the peptide toxins ω-conotoxin GVIA (ω-CgTx) and ω-Aga-IVA, respectively.

Such a classification scheme requires that a highly selective agent be available for each channel type. However, DHPs modify electrophysiologically distinct channels in neurons and in skeletal, cardiac, and smooth muscle (Almers & McCleskey, 1984; Adams & Beam, 1989; Bean, 1989; Cohen et al., 1992a; Forti & Pietrobon, 1993), indicating many subtypes of L-type Ca channels. Likewise, ω-CgTx blocks several distinct types of Ca channels that differ in rates of inactivation or in sensitivity to toxin block (Artalejo et al., 1992; Wang et al., 1992). Finally, this classification scheme is incomplete since the number of cloned Ca channels is increasing faster than pharmacological probes can be developed (Snutch & Reiner, 1992). Therefore, additional ligands with different specificities or at least different relative affinities for Ca channel types would be very helpful.

During the purification of ω-Aga-IIIA, we isolated additional toxins that are homologous to this peptide and constitute the family of type III ω-agatoxins. Although their concentrations in the venom are variable and generally fairly low, several additional members of this family were purified in sufficient quantity for pharmacological studies. We have examined the effects of these new toxins on N-, L-, and T-type Ca channels to determine if they could help in the further characterization of these channel types. Some of these toxins show over 100-fold selectivity for N-type over L-type Ca channels, in contrast to ω-Aga-IIIA, which blocks both Ca channels equally well. The newly discovered type III

* To whom correspondence should be addressed at Merck Research Laboratories, R80N-31C, P.O. Box 2000, Rahway, NJ 07065. Telephone: (908) 594-7013. Fax: (908) 594-3925. Internet: mchardy_smith@merck.com.

‡ Department of Membrane Biochemistry and Biophysics, Merck Research Laboratories.

§ Departments of Entomology and Neuroscience, University of California.

∥ Department of Analytical Biochemistry, Merck Research Laboratories.

® Abstract published in *Advance ACS Abstracts,* April 1, 1994.

[1] Abbreviations: ω-CgTx, ω-conotoxin GVIA; ω-Aga-IIIx, type IIIx ω-agatoxin; DHP, 1,4-dihydropyridine; HPLC, high-pressure liquid chromatography; MALDI-TOF-MS, matrix-assisted laser desorption ionization time of flight mass spectrometry.

0006-2960/94/0433-5098$04.50/0

ω-agatoxins might help define and differentiate among the high-affinity toxin binding sites on L-type and N-type Ca channels. A preliminary report of part of this work has been published (Ertel et al., 1992).

MATERIALS AND METHODS

Materials. *Agelenopsis aperta* venom was purchased from Spider Pharm (Feasterville, PA). ^{125}I-ω-CgTx GVIA was purchased from New England Nuclear. Dihydroxybenzoic acid was purchased from Aldrich, and bovine insulin and horse heart cytochrome *c* were from Sigma. Endoproteinases Arg-C, Lys-C, and Asp-N were purchased from Boehringer Mannheim (Germany), and Staph Protease (Glu-C) was from Worthington Biochemical Co. (Freehold, NJ).

Toxin Purification. Venom was fractionated and toxins isolated using reverse-phase and cation-exchange columns, following methods similar to those previously described (Adams et al., 1990; Bindokas et al., 1991; Mintz et al., 1992b): 200–500 μL of venom was thawed and diluted 10-fold in 10 mM trifluoroacetic acid. The fine precipitate was removed by centrifugation at 14000*g* for 2 min (Brinkmann Model 5415). The solvents for the first chromatographic step in toxin purification were 10 mM trifluoroacetic acid in water (A solvent) and 9 mM trifluoroacetic acid in (2:1 v/v) acetonitrile/1-propanol (B solvent). The venom supernatant was loaded at 2 mL/min onto a phenyl column (1.0 × 25 cm, Vydac, The SEP/A/RA/TIONS GROUP, Hesperia, CA) that had been equilibrated at 5% B. After the supernatant was loaded, flow was increased to 4.5 mL/min over the first minute and then the percentage of B was linearly increased from 5% to 20% from 4 to 20 min. From 20 to 95 min, B was linearly increased from 20% to 33%, at which time all components of interest had eluted. The column was washed for 5 min at 99% B. Fractions of 12 mL were generally collected, and the eluent absorbance was monitored at 230 nm through a 1-mm path-length flow cell. The solvents were pumped by two ABI 400 pumps (Applied Biosystems Inc., Foster City, CA); gradient control and absorbance detection were carried out by an ABI 783A absorbance monitor.

The absorbance signal was digitized at 50 Hz at different gains using a National Instruments NB-MIO-16XL board controlled by a program written in the LabView programming language (V 2.2.1, National Instruments, Austin, TX), all on a Macintosh. The data were filtered by retaining the median value of every 25 data points at the highest gain on scale. Data for absorbance, B pump back-pressure, programmed gradient, fraction collector advance times, and injection times were collected and written out to an ASCII file. Post-run analysis of the data was carried out using the graphing program Igor (V 1.25; Lake Oswego, OR).

Fractions were lyophilized and reconstituted for biological testing in 150 mM NaCl, 5 mM KCl, and 10 mM Na-HEPES, pH 7.2, at 1 μL/μL of original venom or venom equivalent. Fractions were tested for the capacity to inhibit ^{125}I-ω-CgTx binding to rat brain synaptic membranes, for the capacity to inhibit $^{45}Ca^{2+}$ influx into chick brain synaptosomes, and/or for the capacity to inhibit ionic currents through Ca channels (see below). Appropriate fractions were pooled, diluted 4-fold with water, and subjected to cation-exchange chromatography (CX-300, 4.6 × 220 mm, ABI). The diluted pool was loaded at 20 mM ammonium acetate (pH 6.2) at 1.25 mL/min and eluted using a 0.9 M/h gradient of ammonium acetate. The absorbance at 280 nm through an 8-mm path-length flow cell was measured. Appropriate fractions were subjected to further chromatography using a C4 column (4.6 × 250 mm, Vydac) and eluted with 0.1% heptafluorobutyric acid both in water (A solvent) and in acetonitrile (B solvent). During the C4 chromatography step, the flow rate was 1.2 mL/min, and the programmed gradient was composed of the following linear segments: 10% B from 0 to 4 min, to 33% B at 15 min, and then to 48% B at 45 min. Some fractions were then chromatographed using a C18 column (4.6 × 250 mm, Vydac) and eluted with 10 mM trifluoroacetic acid in water (A solvent) and with 9 mM trifluoroacetic acid in acetonitrile (B solvent). During the C18 chromatography step, the flow rate was 1.25 mL/min, and the programmed gradient was run with the following linear segments: 10% B from 0 to 4 min, to 23% B at 14 min, and then to 30% B at 35 min. For both the C18 and the C4 column steps, absorbance was measured at 230 nm through an 8-mm path-length flow cell.

Protein Chemistry. Structural characterization was carried out by subjecting purified toxins to N-terminal sequencing, matrix-assisted laser desorption ionization time-of-flight mass spectrometry (MALDI-TOF-MS), and/or reduction and alkylation using iodoacetic acid.

For reduction and alkylation using iodoacetic acid, 0.2–2 nmol of purified toxin was reduced in 50 μL of 6 M guanidine hydrochloride, 1 mM ethylenediaminetetraacetate, 5 mM dithiothreitol, and 100 mM Tris-HCl, pH 9.3, under argon at 56 °C for 2 h. An equal volume of 6 M guanidine hydrochloride, 1 mM ethylenediaminetetraacetate, 20 mM iodoacetic acid, and 700 mM Tris-HCl, pH 8, was then added; the samples were incubated in the dark for 1 h at room temperature. Samples were desalted using a 25-min gradient across a C18 column. Carboxymethylated toxins were dried and subjected to N-terminal sequencing and/or peptide mapping and sequencing.

To carry out peptide mapping, 0.1 nmol of toxin was incubated with 0.3–1 μg of either endoproteinase Lys-C, Arg-C, Glu-C, or Asp-N, in 100 μL of 100 mM sodium phosphate, pH 8.0, for 4 days at 37 °C. Peptide fragments were separated using a 0.21 × 15 cm C18 column (Vydac) on an ABI 130 HPLC with an ABI 1000S diode array detector. Absorbances at 210, 230, 256, and 280 nm were monitored; the same data collection system described above was used.

To determine N-terminal sequences, intact toxins or peptide fragments were dried onto Porton glass fiber protein or peptide supports (Beckman, Fullerton, CA); Edman degradation was performed using a Porton 2090E microsequencer. Phenylthiohydantoin amino acid derivatives were separated using the on-line Hewlett Packard 1090 HPLC system. Repetitive yields for the instrument were typically in the range 88–96%.

For mass spectrometry, a 0.5-μL aliquot of sample was added to 0.5 μL of a saturated dihydroxybenzoic acid solution (about 50 mM) in water on the sample target surface (stainless-steel, 12-mm diameter). Solvent was removed by drying under a stream of air. Bovine insulin ($M+H^+$ = 5734.5 Da, 0.5 pmol) and horse heart cytochrome *c* ($M+H^+$ = 12 361 Da, 0.4 pmol) in 0.5 μL of water were added as calibrants to the dried sample, and this mixture was dried again. All mass spectra were recorded using a Finnigan MAT Vision 2000 matrix-assisted laser desorption time-of-flight mass spectrometer (Finnigan Corp., San Jose, CA). The Vision 2000 was equipped with an LSI VSL-337 ND nitrogen laser (337 nm), CCD video camera with monitor, ion mirror, 5-keV ion source, and 20-keV postacceleration detector. Up to 12 samples were loaded onto the sample target, and samples were irradiated with the 337-nm beam. Signal transients were recorded with a time resolution of 5 ns. Typically, spectra

were generated from the sum of 5–10 laser pulses, and masses were measured as peak centroids.

Using the above purification protocol, contamination of a given sample of ω-Aga-IIIA, ω-Aga-IIIB, or ω-Aga-IIID by another known type III ω-agatoxin was always less than 1%, using N-terminal sequencing and mass spectrometry to estimate contamination. Nevertheless, it is possible that we have overestimated the potency of ω-Aga-IIIB and ω-Aga-IIID at blocking L-type Ca channels because of very low levels of contamination by the more potent ω-Aga-IIIA. We think this is unlikely because the chromatographic resolution of the "base" subtypes was excellent. For example, the fraction from the C4 column containing ω-Aga-IIIB, when separated on the C18, still showed near-base-line resolution of the small amount of contaminating ω-Aga-IIIA-58T from ω-Aga-IIIB (see Results and Figure 1E). Similarly, ω-Aga-IIID was well resolved from the other two "base" subtypes during the cation-exchange step. Cross-contamination of the variants of ω-Aga-IIIA or ω-Aga-IIIB was more problematic; it was dependent on the fraction cuts made at the last stage of purification and could be significant (>10%).

Binding Studies. The binding of ^{125}I-ω-CgTx to rat brain synaptic membranes was carried out similarly to methods previously described (Feigenbaum et al., 1988), with modifications made necessary by the use of solutions containing higher salt concentrations. Membranes (3 μg of protein per assay tube) were incubated for 3 h at room temperature in 0.2 mL of 150 mM NaCl, 5 mM KCl, 10 mM Na-HEPES, pH 7.5, and 30 pM ^{125}I-ω-CgTx, without or with venom fractions or purified toxins. Venom fractions were tested at a final dilution of 1:30 000 original venom volume. Non-specific binding was defined by binding of ^{125}I-ω-CgTx in the presence of 10 nM ω-CgTx. All binding assays included 0.1% bovine serum albumin. Bound ligand was separated from free by filtration through GF/C filters (Whatman) that had been presoaked in 0.5% polyethylenimine; after sample filtration, the filter was washed twice with 3 mL of 200 mM NaCl and 10 mM Na-HEPES, pH 7.5. Duplicate or triplicate samples were obtained for each experimental condition, and the data were averaged. The standard deviation or the half-range of the replicates was typically less than 3% of the mean.

Synaptosomal $^{45}Ca^{2+}$ Uptake. Synaptosomes were prepared from whole brain tissue (minus brain stem) of 2–5-day-old white leghorn chicks (Charles Sullivan) according to previously reported procedures (Venema et al., 1992) with the following modifications. Brain tissue was homogenized in sucrose–HEPES buffer (in mM: sucrose, 320; HEPES, 20; pH 7.4) at 3000 rpm using a Wheaton glass/Teflon homogenizer. The homogenate was centrifuged at low speed (4300 rpm, Beckman JA-20 rotor) for 10 min to yield a P1 pellet. The pellet was discarded, and the supernatant was recentrifuged at 12500*g* for 20 min to obtain a P2 pellet. This pellet was resuspended in Ca-free, low-K solution (in mM: KCl, 5; $MgCl_2$, 1.4; NaH_2PO_4, 1.2; glucose, 10; choline chloride, 145; HEPES, 20; pH 7.4) to a protein concentration of 1–2 mg/mL. Varying concentrations of toxin were added to the suspension, with 0.5 mg/mL lysozyme as a carrier protein. After incubation for 30 min, the suspension was combined with high-K solution (in mM: KCl, 137; choline chloride, 13; $MgCl_2$, 1.4; NaH_2PO_4, 1.2; glucose, 10; HEPES, 20; $CaCl_2$, 1; pH 7.4). The final concentration of K^+ was 70 mM. The reaction was stopped after 5 s by the addition of 2 mL of terminating solution (in mM: EGTA, 30; choline chloride, 120; KCl, 5; pH 7.4), and the solution was then rapidly filtered using a Skatron cell harvester. The filters were washed for 20 s with washing solution (in mM: KCl, 5; choline chloride, 145; $MgCl_2$, 1.4; $CaCl_2$, 1; HEPES, 20; pH 7.4) and then placed in 1 mL of scintillant (Liquiscint). Radioactivity was counted and used as a measure of $^{45}Ca^{2+}$ entry into synaptosomes; counts from low-K tubes were subtracted from high-K tubes to obtain the voltage-sensitive fraction of $^{45}Ca^{2+}$ entry.

Housefly Neuromuscular Transmission. Toxins were tested for antagonism of housefly neuromuscular transmission in longitudinal ventrolateral muscles of late third instar housefly larvae (*Musca domestica*) as described previously (Adams et al., 1989; Bindokas & Adams, 1989). Larvae were chosen 1–1.5 h following pupariation, at which stage the neurally-evoked twitch responses in these muscles are minimal, yet electrical properties remain intact. After dissection and evisceration, muscles were bathed in physiological saline containing (in mM): NaCl, 140; KCl, 5; $CaCl_2$, 0.75; $MgCl_2$, 1; $NaHCO_3$, 4; HEPES, 5; pH 7.0. Segmental nerves were stimulated with a suction electrode, and excitatory junctional potentials were recorded intracellularly with glass micropipets. Toxins were dissolved in the above saline and applied by bath perfusion. Muscles 6A and 7A of the fourth segment were used in all experiments.

Whole Cell Voltage Clamp Measurements. Isolated atrial myocytes were prepared from male Duncan–Hartley guinea pigs as described previously (Mitra & Morad, 1985; Cohen et al., 1992b). The procedure for isolating soma of locust (*Schistocerca americana*) thoracic neurons was similar to that described by Suter and Usherwood (1985), except that neurons were isolated from both the metathoracic and mesothoracic ganglia and mechanical disruption of the ganglia was more extensive in order to obtain cell surfaces suitable for gigaohm seal formation.

The methods used for patch voltage clamp experiments in the whole cell configuration have been described previously (Ertel et al., 1994). The internal (pipet) solution usually contained the following (in mM): cesium glutamate, 107; CsCl, 20; tetrabutylammonium chloride, 1; 1,2-bis(2-aminophenoxy)ethane-*N*,*N*,*N*′,*N*′-tetraacetic acid (BAPTA), 11; $CaCl_2$, 0.9; $MgCl_2$, 1; HEPES, 20; Mg-ATP, 5; Li_2-GTP, 0.1; pH 7.2 with CsOH. For some experiments with locust neurons, the cesium glutamate was replaced by CsCl. The external (bath) solution usually contained the following (in mM): tetraethylammonium chloride, 157; $CaCl_2$, 5; $MgCl_2$, 0.5; HEPES, 10; pH 7.5 with CsOH; and 0.05% fatty acid free bovine serum albumin (Boehringer Mannheim). For some experiments with locust neurons, the $CaCl_2$ was replaced with 2 mM $BaCl_2$, and the concentration of tetraethylammonium chloride was increased to 162 mM. Solutions were pressurized with 100% O_2 and experiments were conducted at room temperature (20–25 °C).

Membrane current was low-pass-filtered using a four-pole Bessel filter with a cutoff frequency (f_c, −3 dB) of 5 kHz and digitized at 40 kHz. Linear leak and capacity currents were subtracted digitally by scaling the average response to 16 test pulses from −100 to −140 mV. Zero Ca current was defined as the current at the holding voltage and is indicated by a dashed line in figures with current recordings. Changes in membrane voltage were complete within 250 μs after a change in command voltage, unless stated otherwise, and data points collected during this "blanking" period were excluded from analysis and display. Tail currents were fit by the sum of two exponentials plus a constant, and the reported tail current amplitudes represent the magnitude of the exponentials at the end of the "blanking" period.

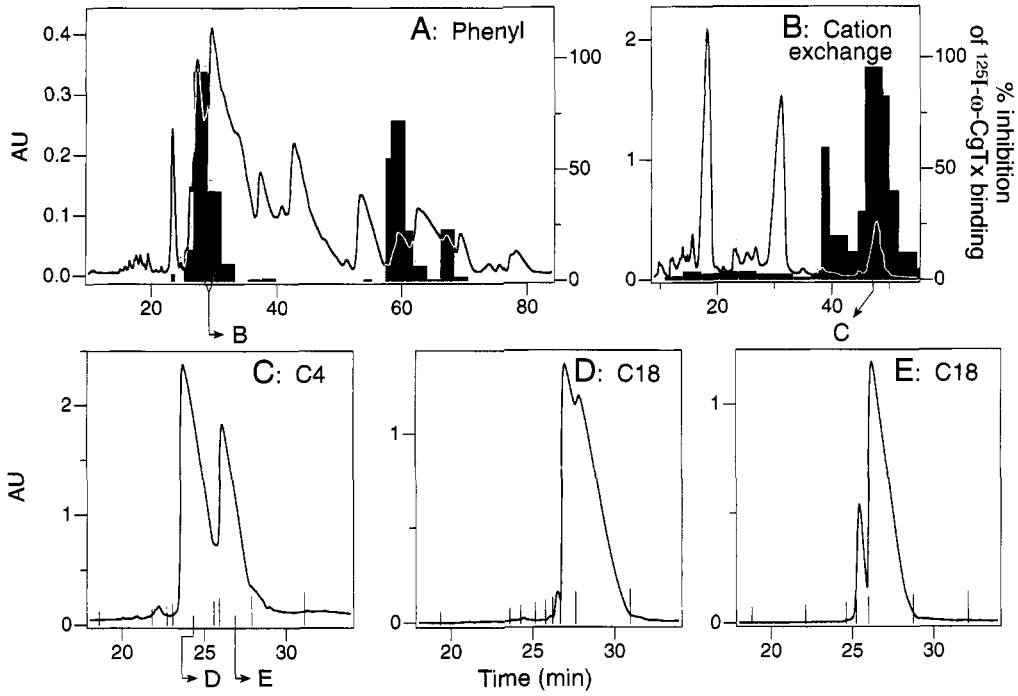

FIGURE 1: Purification of ω-Aga-IIIA, ω-Aga-IIIB, and ω-Aga-IIID. (A) Venom (480 μL) was loaded onto a 1 × 25 cm phenyl column. Proteins were eluted using a gradient from aqueous to organic as described in Materials and Methods, and the absorbance of the eluent was measured at 230 nm (continuous trace, left scale). Fractions were tested for the capacity to inhibit ^{125}I-ω-CgTx binding to rat brain synaptic membranes (bars, right scale). (B) The indicated fractions from the phenyl column were pooled with equivalent fractions from similar purifications, and a total of 990 μL of venom equivalents was loaded onto a CX-300 cation-exchange column. Proteins were eluted using a gradient of ammonium acetate, pH 6; fractions were tested as above. (C) The fraction indicated was applied to a C4 column and eluted using a linear gradient from aqueous to organic. (D, E) The two fractions indicated were applied to separate C18 runs, yielding ω-Aga-IIIA and ω-Aga-IIIB, respectively. The samples were eluted using a linear gradient from aqueous to organic. The fractions from panel D were ω-Aga-IIIA and a variant of ω-Aga-IIIA, while the major peak eluting in panel E was ω-Aga-IIIB (the small peak eluting in front of the ω-Aga-IIIB was ω-Aga-IIIA-58T). The fraction eluting from the cation-exchange column (panel B) at 38 min, which inhibited ^{125}I-ω-CgTx binding, was also further purified (not shown), sequenced, and named ω-Aga-IIID. The fractions collected after that indicated in panel B (49–52 min) were also subjected to the C4 and C18 purification steps: the purified toxins were principally ω-Aga-IIIB variants.

To determine the dose–response curves for block of L-type Ca current in atrial myocytes, two methods were used to correct for the unblocked components. For ω-Aga-IIIA, maximally active concentrations were applied, and the unblocked portions of the sustained inward current and the rapidly decaying tail current were measured. The remaining sustained inward current represented 12% ± 4% (SEM, n = 13) of the initial current in all cases, and it was attributed to T-type Ca channels (Cohen et al., 1992a; Ertel et al., 1994). Similarly, the remaining unblocked fast tail current (37% ± 3%, SEM, n = 13) was attributed to gating currents (Ertel et al., 1994). These unblocked components were subtracted from the current magnitudes measured in various toxin concentrations to yield the contribution of ionic currents through L-type Ca channels. For ω-Aga-IIIB and ω-Aga-IIID, since the higher EC_{50} values and the scarcity of the toxins rendered the application of maximally active concentrations difficult, we assumed that the contribution of the unblocked components was the same as that found on average for ω-Aga-IIIA.

RESULTS

Toxin Purification and Structural Characterization. During the purification of ω-Aga-IIIA, we found a number of related toxins that inhibit ^{125}I-ω-CgTx binding and have similar chromatographic retention times on various matrices. Some of these toxins inhibit the binding of ^{125}I-ω-CgTx to N-type Ca channels with a potency similar to that of ω-Aga-IIIA, but they block L-type Ca channels less potently than ω-Aga-IIIA. As an approach to the identification of structural features necessary for high-potency L-type Ca channel block, we characterized these related toxins. Pharmacological characterization will be presented following the purification and structural characterization.

Whole *Agelenopsis aperta* venom was fractionated by reverse-phase HPLC across a phenyl matrix (Figure 1A), and the fractions were assayed for the ability to inhibit the binding of ^{125}I-ω-CgTx to rat brain synaptic membranes. This activity elutes in two well-separated regions. The first peak contains type III ω-agatoxins while later peaks of activity contain type II ω-agatoxins (unpublished results). The two fractions containing most of the activity from the earlier peak were pooled with those from two similar purifications and chromatographed using a cation-exchange matrix (Figure 1B). The resulting chromatogram has two distinct regions. In the first region, two proteins of high abundance elute, which do not inhibit the binding of ^{125}I-ω-CgTx to rat brain synaptic membranes. By N-terminal sequencing and electrospray mass spectrometry, we identified these proteins as the previously characterized μ-Aga-IV, eluting at 18 min, and μ-Aga-II, eluting at 30 min (Skinner et al., 1989). Proteins that do inhibit ^{125}I-ω-CgTx binding start to elute at 38 min, and most of the activity appears as a peak with multiple inflection points between 44 and 50 min.

We further purified the fraction with greatest activity using a C4 matrix (Figure 1C). The activity separates into two major peaks, both of which inhibit ^{125}I-ω-CgTx binding to rat brain synaptic membranes with approximately equal potency (see below). Each peak was further fractionated over a C18 matrix (Figure 1D,E). The major peaks in panels D and E of Figure 1 contain ω-Aga-IIIA and ω-Aga-IIIB, respectively

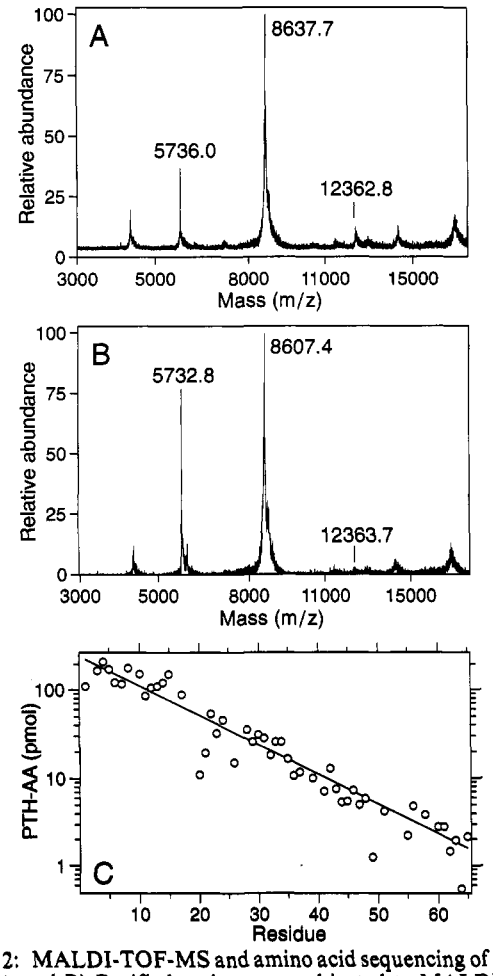

FIGURE 2: MALDI-TOF-MS and amino acid sequencing of ω-Aga-IIIB. (A and B) Purified toxins were subjected to MALDI-TOF-MS. The centroided molecular mass was 8637 Da (A) or 8607 Da (B), calibrated using the standards insulin and cytochrome *c*. All major peaks in the spectra could be accounted for by m/z, $m/2z$, or $2m/z$ of the sample or the calibrants. (C) ω-Aga-IIIB was applied to a Porton peptide glass fiber filter, and automated Edman degradation was carried out using a Porton 2090E microsequencer. The amount of detected phenylthiohydantoin amino acid derivative, after subtraction of background for that residue from the prior cycle, is plotted versus cycle number. The line is an exponential fit to the data with a repetitive yield of 92%.

(see below). We were particularly interested in the toxin comprising the major peak shown in Figure 1E because it blocked N-type Ca channels with the same potency as ω-Aga-IIIA but was less potent in blocking L-type Ca channels. Succeeding fractions eluting from the cation-exchange column were found to have the same activity profile and were also purified. Samples with this activity profile had the same N-terminal sequence for 28 residues, and this sequence differed from that of ω-Aga-IIIA at 2 positions: an Ile to Phe substitution at position 5 and an Arg to Ser substitution at position 21. MALDI-TOF-MS of different samples with this N-terminal sequence showed the presence of three proteins with molecular masses of 8581, 8607, and 8637 Da (e.g., Figure 2A,B and Table 1). A longer N-terminal sequence was obtained from reduced and carboxymethylated samples and from native samples derived for the 8607-Da and 8581-Da toxins; the yield of the various PTH-amino acid derivatives from one sequencing run is shown in Figure 2C, the amino acid sequences called are shown in Figure 3A. The 2 samples with molecular masses of 8607 and 8581 Da were identical for 37 residues, with the exception of a Ser/Asn difference at position 29.

The complete sequence of ω-Aga-IIIB was assembled from overlapping peptide fragments and the N-terminal sequence data (Figure 3B). Using a sample of molecular mass of 8607 Da with a contaminating mass of 8637 Da, we observed 10 differences between the sequences of ω-Aga-IIIB and ω-Aga-IIIA (Figure 3C). In the sequencing of the peptides, both a Lys and an Arg were detected at position 35 (Figure 3B). The Lys at position 35 was also detected in the longer sequencing run (Figures 2C and 3A); the presence of Arg at position 35 was confirmed by the sequencing of a peptide from positions 36 to 49 in the Endo Arg-C cleavage reaction. The difference in the molecular mass of Lys and Arg (28 Da) accounts for the difference in the molecular mass of the two toxins present in the sample (30 Da). Apart from the Arg at position 35, all residues were called from a minimum of two separate sequencing runs. The C-terminal Arg was called in three independent runs from the Glu-C and the Asp-N digestions.

Thus, we have purified a (29S,35K)ω-Aga-IIIB (8581 Da), a (29N,35K)ω-Aga-IIIB (8607 Da), and a (29N,35R)ω-Aga-IIIB (8637 Da) (Figure 3C and Table 1). To simplify and because we have extensively characterized the sequence of (29N,35K)ω-Aga-IIIB, we call this variant "base" ω-Aga-IIIB (Table 1). The other two variants are then named relative to it: (29S,35K)ω-Aga-IIIB becomes ω-Aga-IIIB-29S (the 29S denoting the change from the ω-Aga-IIIB sequence) and (29N,35R)ω-Aga-IIIB becomes ω-Aga-IIIB-35R (Figure 3C).

The first major peak from the C4 column is ω-Aga-IIIA. This fraction, when run on a C18 column, produces an asymmetric peak (Figure 1D). We characterized in detail the components of the two fractions isolated from this peak. Edman degradation produced identical N-terminal amino acid sequences for 30 residues, which matches the sequence previously published for ω-Aga-IIIA (Venema et al., 1992). However, MALDI-TOF-MS showed that the major component of the front portion of the peak has a molecular mass of 8505 Da, identical to that of ω-Aga-IIIA (Venema et al., 1992), whereas the major component of the back portion has a molecular mass of 8478 Da.

To understand this apparent discrepancy, we obtained partial amino acid sequences for the two toxins using proteolytic digestion. From the toxin in the front portion of the peak, we obtained, among others, a peptide with the sequence ARQCYN, corresponding to residues 56–61 of ω-Aga-IIIA. From the toxin in the back portion of the peak, we obtained, with Endo Glu-C, a peptide with the sequence FQGICRRKARTCYNSDPDKC, corresponding nearly exactly to residues 48–67 of ω-Aga-IIIA, except for the Gln to Thr substitution at position 58. The difference in the molecular mass of Gln and Thr (27 Da) accounts for the difference of 27 Da between the two toxins. Therefore, the front of the C18 peak is "authentic" ω-Aga-IIIA as previously described (Venema et al., 1992), whereas we designate the toxin eluting later as ω-Aga-IIIA-58T (Table 1). The smaller peak in front of the main ω-Aga-IIIB peak depicted in Figure 1E is also ω-Aga-IIIA-58T, as determined by mass spectrometry and N-terminal sequencing. The two forms of ω-Aga-IIIA showed no difference in the capacity to inhibit ^{125}I-ω-CgTx binding to the N-type Ca channel in rat brain synaptic membranes nor in the capacity to block L-type Ca currents in guinea pig atrial myocytes (not shown). Assuming 100% recovery of ω-Aga-IIIA and ω-Aga-IIIA-58T through all stages of the purification, these toxins are present in venom at approximately 15 and 20 μM, respectively. We have also detected a third species with the same N-terminal sequence as ω-Aga-IIIA for 30 residues, but with a molecular mass of 8484 Da (V.A.W.,

A: N-terminal sequence

```
Mass                    .         .        ⇓.         .         .         .
8607   S IDFGGD DGEKDD Q  RSNGY S YNLFGYLKSG K EVGTSAEFR I   KA Q YNSDPD  V
8581   SCIDFGGDCDGEKDDCQCCRSNGYCSCYSLFGYLKSG
```

B: Endoprotease digestion sequences

```
                .         .         .         .         .         .         .
       SCIDFGGDCDGEKDDCQCCRSNGYCSCYNLFGYLKSGCKCEVGTSAEFRRICRRKAKQCYNSDPDKCVSVYKPKRR
N-Term <-------------------------*-------------------------------------->
Asp N            <------>       <-----*-------->  <-------->          <---------->
Lys C  <---------> <------>              <------------------->       <------>
Glu C  <------------------>        <->              <------------------>  <------>
Arg C  <------------------>              <-------------><---><------------------>
```

C: Homology between the ω-Aga-III variants

```
                        .         .         .         .         .         .          Mass
ω-Aga-IIIA      SCIDIGGDCDGEKDDCQCCRRNGYCSCYSLFGYLKSGCKCVVGTSAEFQGICRRKARQCYNSDPDKCESHNKPKRR   8505
ω-Aga-IIIA-58T  SCIDIGGDCDGEKDDCQCCRRNGYCSCYSLFGYLKSGCKCVVGTSAEFQGICRRKARTCYNSDPDKCESHNKPKRR   8478
ω-Aga-IIIB-35R  SCIDFGGDCDGEKDDCQCCRSNGYCSCYNLFGYLRSGCKCEVGTSAEFRRICRRKAKQCYNSDPDKCVSVYKPKRR   8637
ω-Aga-IIIB      SCIDFGGDCDGEKDDCQCCRSNGYCSCYNLFGYLKSGCKCEVGTSAEFRRICRRKAKQCYNSDPDKCVSVYKPKRR   8607
ω-Aga-IIIB-29S  SCIDFGGDCDGEKDDCQCCRSNGYCSCYSLFGYLKSGCKCEVGTSAEFRRICRRKAKQCYNSDPDKCVSVYKPKRR   8581
PTX1      AELTSCFPVGHECDGDASNCNCCGDDVYCGC----GWGRWNCKCKVADQSYAYGICKDKV-NCFNRHLWPAKVCKKPCRREC   8571
ω-Aga-IIIC      NCIDFGGDCDGEKDDCQCCXRNGYCSCYNLFGYLKRGCKXEVG...                                  8638
ω-Aga-IIID      SCIKIGFDCDGDKDDCQCCRTNGYCSXYXLFGYLKSG...                                        9167
```

FIGURE 3: Amino acid sequences of the type III ω-agatoxins. (A) Determination of the N-terminal sequence of two variants of ω-Aga-IIIB. The 8607-Da variant was sequenced without prior reduction and carboxymethylation; thus, the PTH-Cys derivatives were not called (though principal peaks related to PTH-Cys were detected in all appropriate cycles); the yield of PTH-amino acid derivatives from this sequencing run is shown in Figure 2C. The 8581-Da variant was reduced and carboxymethylated before sequencing. The arrow points to the 29th position, which was an Asn in the 8607-Da variant and a Ser in the 8581-Da variant. We call the two variants ω-Aga-IIIB and ω-Aga-IIIB-29S, respectively. (B) Determination of the full sequence of ω-Aga-IIIB. A 0.5-nmol aliquot of ω-Aga-IIIB (molecular mass 8607 Da with contaminating 8637 Da) was reduced and carboxymethylated, and 0.1-nmol aliquots were cleaved with residue-specific endoproteinases. The fragments generated were separated and sequenced. From this information, the complete sequence was deduced. The asterisk at position 29 indicates the position of the Ser/Asn variation seen above; the asterisk at position 35 indicates a position where both Arg and Lys were seen (see text). (C) Alignment of the amino acid sequences of the two variants of ω-Aga-IIIA and three variants of ω-Aga-IIIB, along with the partial sequences of ω-Aga-IIIC and ω-Aga-IIID and the sequence of Tx1 from *Phoneutria nigriventer* (Diniz et al., 1990). Identical residues are enclosed.

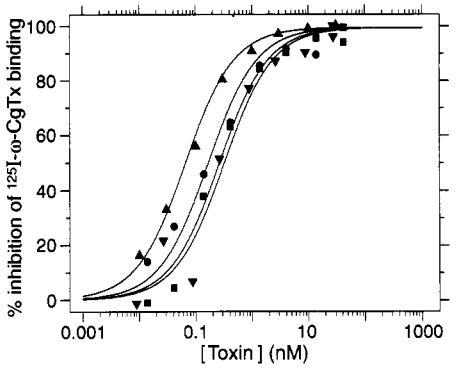

FIGURE 4: Dose–response relationships for inhibition of ^{125}I-ω-CgTx binding to rat brain synaptosomes by type III ω-agatoxins compared to ω-CgTx. The nonspecific binding was subtracted, and the Michaelis–Menten fits assume 1 to 1 binding. The calculated IC_{50} values are as follows: (▲) ω-CgTx, 67 pM; (●) ω-Aga-IIIA, 170 pM; (■) ω-Aga-IIIB, 220 pM; (▼) ω-Aga-IIID, 330 pM.

M.E.A., and M.M.S., unpublished results); the full sequence of this third variant of ω-Aga-IIIA has not been determined.

In one purification of raw venom, we isolated another member of the ω-Aga-III family. N-Terminal sequencing of this toxin produced a sequence sufficiently different from ω-Aga-IIIA or ω-Aga-IIIB to justify the name ω-Aga-IIIC (Figure 3C). This toxin was not found in subsequent purifications and thus was not characterized further.

We also purified the fraction eluting at 38 min from the cation-exchange column (Figure 1B) on a C18 matrix (chromatogram not shown); this fraction significantly inhibited the binding of ^{125}I-ω-CgTx to its receptor. The N-terminal amino acid sequence was determined by Edman sequencing (Figure 3C), and the molecular mass of 9167 Da was determined by MALDI-TOF-MS. Although adequate amounts of this toxin were not available for full sequence determination, it is clear that the N-terminal sequence differs substantially from that of the variants of ω-Aga-IIIA, ω-Aga-IIIB, or ω-Aga-IIIC, and we named this toxin ω-Aga-IIID.

Effects of ω-Aga-IIIA, ω-Aga-IIIB, and ω-Aga-IIID on Ca Channels. (A) Effects on N-Type Ca Channels in Rat and Chick Brain Membranes. ω-Aga-IIIA, ω-Aga-IIIB, and ω-Aga-IIID are equipotent on N-type Ca channels. All three toxins completely inhibit the binding of ^{125}I-ω-CgTx to rat brain synaptic membranes (Figure 4). The IC_{50} values for the three ω-agatoxins are similar (170–330 pM) and only slightly greater than that for ω-CgTx itself (67 pM). We never detected a difference in potency of more than 2-fold between the variants of ω-Aga-IIIA or ω-Aga-IIIB in these binding experiments. All three type III ω-agatoxins block K^+-stimulated $^{45}Ca^{2+}$ entry into chick brain synaptosomes (Figure 5), an assay for Ca flux through ω-CgTx-sensitive Ca channels. As previously documented (Venema et al., 1992), block by ω-Aga-IIIA is partial (54%), when compared to ω-CgTx (80%). Likewise, ω-Aga-IIIB partially blocks Ca^{2+} entry (52%). As quantities of ω-Aga-IIID were limited, it could not be tested at saturating concentrations, but the data fit a model where it blocks approximately the same fraction of Ca uptake (77%) as did ω-CgTx. The estimated IC_{50} value for ω-Aga-IIIB (1 nM) was close to that of ω-Aga-IIIA (2 nM), but somewhat lower than that of ω-Aga-IIID (35 nM) or ω-CgTx (11 nM).

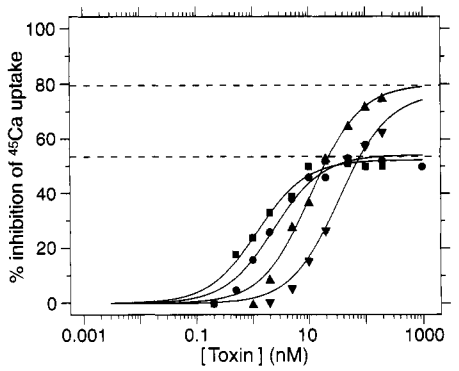

FIGURE 5: Dose–response relationships for block of $^{45}Ca^{2+}$ fluxes into chick brain synaptosomes by the type III ω-agatoxins. The flux in low-potassium medium was subtracted, and the Michaelis–Menten fits assume 1 to 1 binding. The calculated maximal inhibition and IC_{50} values are as follows: (■) ω-Aga-IIIB, 52% and 1.2 nM; (●) ω-Aga-IIIA, 54% and 2.4 nM; (▲) ω-CgTx, 80% and 11 nM; (▼) ω-Aga-IIID, 77% and 35 nM.

(B) Effects on L- and T-Type Ca Channels in Guinea Pig Atrial Myocytes. L- and T-type Ca currents were recorded in freshly isolated guinea pig atrial myocytes with the whole cell variation of the patch voltage clamp technique. ω-Aga-IIIB and ω-Aga-IIID block L-type Ca channels with reduced potency compared to ω-Aga-IIIA (Figures 6 and 7). When cells held at −90 mV are depolarized to +20 mV for 10 ms, an inward calcium current develops, which is sustained during the pulse (Figure 6). This current is a combination of currents through L- and T-type Ca channels, but at +20 mV, the contribution of T-type currents is usually less than 15%. When cells are repolarized to −50 mV, a large inward tail current is observed, which decays with biexponential kinetics. The rapidly decaying component of the tail current represents a combination of ionic and gating currents associated with L-type Ca channels (Cohen et al., 1992a; Ertel et al., 1994). The slowly decaying component reflects the deactivation of T-type Ca channels.

The application of 150 nM ω-Aga-IIID has two distinct effects (Figure 6A). First, the sustained inward calcium current is reduced about 50%, indicating block of L-type Ca channels. Second, the rapidly decaying tail current is reduced about 30%, also consistent with L-type Ca channel block. In contrast, the slowly decaying tail current is unchanged, indicating that T-type Ca channels are unaffected. The transient outward current at the beginning of the test pulse (a combination of Na and Ca channel gating currents) is also unchanged, suggesting that ω-Aga-IIID, like ω-Aga-IIIA (Ertel et al., 1994), does not modify gating charge movements. This result and the fact that channel gating currents contribute on average 37% of the rapidly decaying tail current are consistent with the more pronounced block observed for the sustained inward current than for the rapidly decaying tail current.

The block of Ca currents by ω-Aga-IIIA and ω-Aga-IIIB (Figure 6B,C) is similar to that by ω-Aga-IIID, except for differences in potency. All three toxins specifically block currents through L-type Ca channels without affecting T-type Ca channels or gating currents. The onset of block is relatively fast (under 60 s at the EC_{50}, and under 10 s at maximal concentrations) and poorly reversible (not shown). However, 50% block of L-type Ca channels is obtained with about 150 nM ω-Aga-IIID compared to 60 nM ω-Aga-IIIB and 0.45 nM ω-Aga-IIIA. In this assay, none of the variants of ω-Aga-IIIB or ω-Aga-IIIA has a potency substantially different from that of the appropriate base toxin.

To measure accurately the potencies of block of current through L-type Ca channels, we plotted dose–response relationships for three type III ω-agatoxins (Figure 7). L-Type Ca channel currents were quantified using the magnitude of the sustained inward current at the end of the test pulse as well as that of the rapidly decaying tail current. We corrected these two measurements for the contribution of T-type Ca channel currents and gating currents, respectively (see Materials and Methods). For each of the three toxins, the two dose–response curves obtained in this manner are in good agreement (Figure 7). The EC_{50} for block of L-type Ca currents by ω-Aga-IIIA is about 0.35 nM, consistent with previous reports (Mintz et al., 1991; Cohen et al., 1992a). The correction method used with ω-Aga-IIIB and ω-Aga-IIID introduces some error in the determination of the EC_{50} values (47 nM for ω-Aga-IIIB and 130 nM for ω-Aga-IIID), which are probably less accurate than the one for ω-Aga-IIIA. Despite this limitation, the two new type III ω-agatoxins are clearly over 100 times less potent than ω-Aga-IIIA in

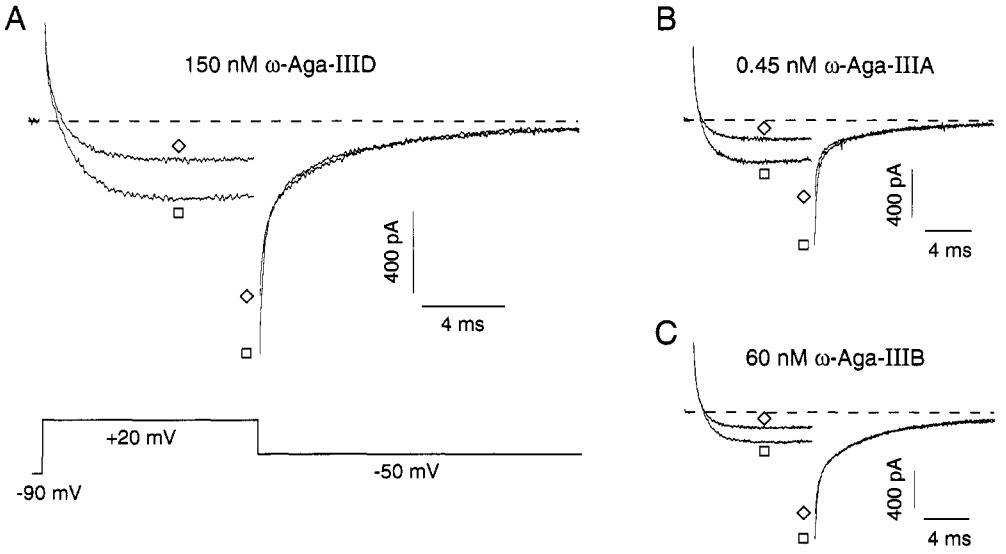

FIGURE 6: Type III ω-agatoxins block Ca^{2+} currents in voltage-clamped guinea pig atrial myocytes. The voltage protocol is shown in the bottom left panel. All three type III ω-agatoxins block L-type Ca channel currents but do not affect T-type Ca channels or gating currents. (□) Control; (◇) +toxin. (A) ω-Aga-IIID, 150 nM; (B) ω-Aga-IIIA, 0.45 nM; (C) ω-Aga-IIIB, 60 nM.

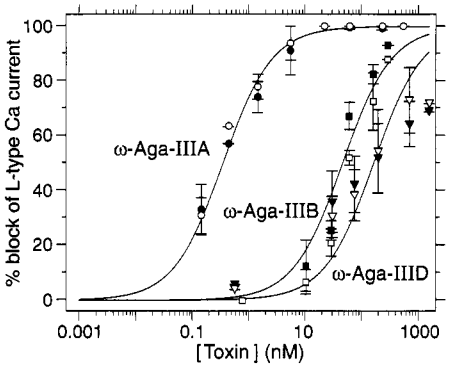

FIGURE 7: Block of L-type Ca channel currents in guinea pig atrial myocytes by type III ω-agatoxins. Block of L-type Ca channel currents was quantified using the changes in the magnitude of the sustained inward current (closed symbols) or the magnitude of the rapidly decaying tail current (open symbols). The two measurements were corrected for T-type Ca channel currents and gating currents, respectively, as described under Materials and Methods. The Michaelis–Menten fits assume 1 to 1 binding. The calculated IC_{50} values are as follows: (●, ○) ω-Aga-IIIA, 0.35 nM; (■, □) ω-Aga-IIIB, 47 nM; (▼, ▽) ω-Aga-IIID, 130 nM.

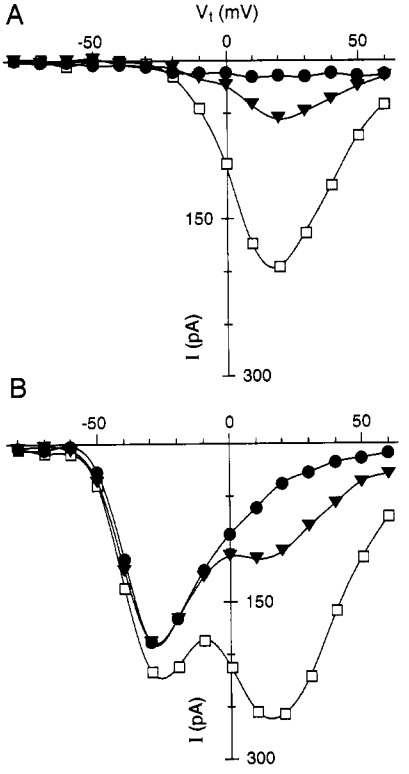

FIGURE 8: Type III ω-agatoxins specifically isolate currents through T-type Ca channels. Current–voltage relationships are plotted for L- and T-type Ca currents with and without ω-Aga-IIID and ω-Aga-IIIA. (A) Holding voltage is –50 mV. (B) Holding voltage is –90 mV. For both panels: (□) control; (▼) 600 nM ω-Aga-IIID; (●) 600 nM ω-Aga-IIID plus 60 nM ω-Aga-IIIA.

blocking L-type Ca channels in guinea pig atrial myocytes. This decrease in potency suggests that the differences in protein sequence among the three toxins significantly affect their recognition of L-type Ca channels.

T-Type Ca channels appear unaffected by type III ω-agatoxins. In Figure 8, we plot current–voltage relationships for the sustained inward current at the end of the test pulse, without or with ω-Aga-IIID and ω-Aga-IIIA. In the experiment depicted in panel A, the holding potential was –50 mV, a voltage that inactivates T-type Ca channels, and the control current–voltage relationship is unimodal, reflecting activation of only L-type Ca channels. The addition of 600 nM ω-Aga-

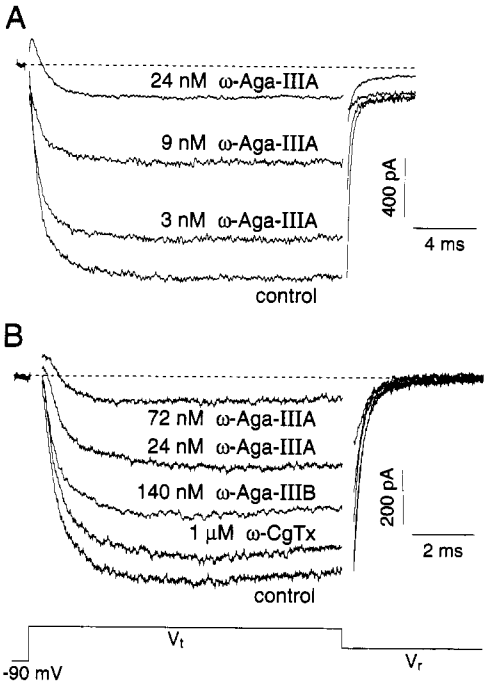

FIGURE 9: Type III ω-agatoxins block locust neuronal Ca channels. The voltage protocol is shown in the bottom panel. (A) Currents recorded from a locust mesothoracic neuron. Test voltage (V_t), –20 mV; repolarization voltage (V_r), –60 mV. The charge carrier was 2 mM Ba, and the pipet solution contained CsCl; 250 μs is blanked after each voltage step. (B) Currents recorded from a locust metathoracic neuron. V_t, +10 mV; V_r, –50 mV; 350 μs is blanked after each voltage step. There were no consistent differences between cells isolated from the two ganglia.

IIID partially blocks these channels in a voltage-independent manner, and the subsequent addition of 60 nM ω-Aga-IIIA completely suppresses the calcium current. In the experiment depicted in panel B, the holding potential was –90 mV, so that both T- and L-type Ca channels were available to open, and the control curve is bimodal, reflecting activation of both types of Ca channels. The peak at negative voltages reflects "low-voltage activated" T-type Ca channels, and the peak at positive voltages reflects "high-voltage activated" L-type Ca channels (Cohen et al., 1992a). The addition of ω-Aga-IIID followed by ω-Aga-IIIA completely suppresses current through L-type channels without affecting current through T-type channels. This result indicates that the toxins, and ω-Aga-IIIA in particular, are useful tools to distinguish between the contribution of currents through L- and T-type Ca channels.

(C) Effects of Type III ω-Agatoxins on Insect Ca Channels. ω-Agatoxins have been defined as type III if they inhibit the binding of ^{125}I-ω-CgTx to vertebrate N-type Ca channels but have no effect at the housefly neuromuscular junction (Bindokas et al., 1991). Indeed, ω-Aga-IIIB and ω-Aga-IIID inhibit ^{125}I-ω-CgTx binding (Figure 4) but have no detectable effect on neuromuscular transmission in housefly body wall muscles, as was found earlier for ω-Aga-IIIA (Bindokas et al., 1991). At concentrations of 100 nM, neither ω-Aga-IIIB nor ω-Aga-IIID had any effect on neurally evoked excitatory junctional potentials (data not shown), whereas the same concentration of ω-Aga-IA reduced the excitatory junctional potentials by 95% [see also Bindokas et al. (1991)]. Since the effects of ω-Aga-IA are attributable to block of presynaptic Ca channels in housefly neurons (Bindokas et al., 1991), some insect neuronal Ca channels are clearly insensitive to block by type III ω-agatoxins.

However, other types of insect neuronal Ca channels are blocked by type III ω-agatoxins (Figure 9). In locust thoracic

Table 1: Abundance, Molecular Mass, and Pharmacological Profile of Type III ω-Agatoxins[a]

toxin	mass (Da)	abundance (μM)	L-type IC_{50} (nM)	N-type ω-CgTx binding IC_{50} (nM)	N-type $^{45}Ca^{2+}$ flux IC_{50} (nM)
ω-Aga-IIIA	8505	15	0.35	0.17	2.4
ω-Aga-IIIA-58T	8478	20			
ω-Aga-IIIB	8607				
ω-Aga-IIIB-29S	8581	≈40	47	0.22	1.2
ω-Aga-IIIB-35R	8637				
ω-Aga-IIIC	8638	0–3	ND	ND	ND
ω-Aga-IIID	9167	3	130	0.33	35

[a] Abundance is the concentration in neat venom, assuming 100% recovery in all steps.

ganglion neurons, ω-Aga-IIIA potently blocks most of the Ca current (80–90%, $n = 8$). The IC_{50} is about 10 nM in the experiment of Figure 9A, indicating a block that is at least 10-fold more potent than any possible block of housefly presynaptic Ca channels. In general, Ca currents recorded from the soma of locust thoracic ganglion neurons were robust and similar to mammalian neuronal "high-voltage-activated" Ca currents, and they were blocked little or not at all by ω-CgTx (Figure 9B). The block of these Ca currents by ω-Aga-IIIA was more potent than by ω-Aga-IIIB ($n = 4$; Figure 9B). In this experiment, 140 nM ω-Aga-IIIB blocked only ≈25% of the current, but 72 nM ω-Aga-IIIA blocked ≈85% of the remaining current.

DISCUSSION

Four pharmacologically distinct classes of peptides that block Ca channels were previously identified in *Agelenopsis aperta* venom. The classification of ω-agatoxins into types I–IV is based on (i) activity in invertebrates, assessed by the block of neuromuscular transmission in houseflies (Adams et al., 1990; Bindokas et al., 1991); (ii) binding to N-type Ca channels in vertebrates, assessed by the inhibition of ω-CgTx binding to chick or rat brain synaptic membranes (Adams et al., 1990; Venema et al., 1992); and (iii) block of P-type Ca channels in vertebrate central neurons (Mintz et al., 1992b). Type I toxins block neuromuscular transmission but are inactive on ω-CgTx binding, type III toxins inhibit ω-CgTx binding but are inactive at the housefly neuromuscular junction, type II toxins are active in both preparations, and type IV toxins are inactive in both preparations but do block P-type Ca channels in mammalian central neurons. We now show that a family of type III ω-agatoxins is present in *A. aperta* venom and these toxins are in turn pharmacologically distinct.

The newly discovered toxins that we have characterized are type III ω-agatoxins by the existing classification scheme: they are inactive at the housefly neuromuscular junction but inhibit ω-CgTx binding. ω-Aga-IIIB and ω-Aga-IIID inhibit high K^+-induced $^{45}Ca^{2+}$ uptake by chick brain synaptosomes (Figure 5) and ^{125}I-ω-CgTx binding to N-type Ca channels (Figure 4) with potencies similar to those of ω-Aga-IIIA.

In Table 1, we summarize the properties of the type III ω-agatoxins, and Figure 3C shows their known amino acid sequences. There are at least seven toxins in this family: two characterized variants of ω-Aga-IIIA, three variants of ω-Aga-IIIB, one variant of ω-Aga-IIID, and one variant of ω-Aga-IIIC. One of the variants of ω-Aga-IIIB has been characterized most extensively. This toxin was sequenced in its entirety (Figure 3B), and the derived sequence is consistent with its mass as determined by MALDI-TOF-MS (Figure 2B). Like ω-Aga-IIIA, ω-Aga-IIIB has 76 amino acid residues, and 66 of the residues are identical between the 2 toxins; in particular, the 12 Cys residues and 22 of the 26 charged amino acid residues are strictly conserved. The cDNA sequences have also been cloned by probing an *A. aperta* venom gland cDNA library (Hillyard et al., 1994). The three cDNAs for ω-Aga-IIIB, ω-Aga-IIIB-29S, and ω-Aga-IIIA-58T show Arg-Arg-Gly as the C-terminal sequence. The protein sequences for ω-Aga-IIIA and ω-Aga-IIIB only show the two identified Arg residues (Figure 3B). ω-Aga-IIIA and ω-Aga-IIIB are probably C-terminally amidated, since the C-terminal Arg is followed by a Gly in the precursors (Hillyard et al., 1994).

ω-Aga-IIIC and ω-Aga-IIID follow the same pattern of amino acid conservation in the portion of their sequence that we have determined, so that most charged residues and all Cys residues are conserved. The combination of the similar IC_{50} values for inhibition of ω-CgTx binding, the similar molecular weights, and the high sequence homology suggests strongly that the three-dimensional structure responsible for the high-potency binding to N-type Ca channels is well conserved among the type III ω-agatoxins.

Interestingly, in a search for homologous proteins, we identified the spider toxin Tx1 from *Phoneutria nigriventer* (Diniz et al., 1990). Tx1 is toxic to vertebrates, but the mechanism of action is unknown. The homology of its sequence with that of the type III ω-agatoxin family is significant: with 2 gaps, there is 34% identity (26 out of 76 residues), including 11 of the 12 Cys residues that are common to the type III agatoxins. This homology suggests that Tx1 may block mammalian Ca channels. If so, its structure might provide clues as to the active face of the type III ω-agatoxins.

Most amino acid substitutions within the type III ω-agatoxin family are conservative, but a few major substitutions are observed (Figure 3C). For example, a positively charged Lys at position 4 in ω-Aga-IIID replaces a negatively charged Asp in ω-Aga-IIIA, ω-Aga-IIIB, and ω-Aga-IIIC. Also, a positively charged Arg at position 21 in ω-Aga-IIIA and ω-Aga-IIIC is replaced by an uncharged Ser in ω-Aga-IIIB and Thr in ω-Aga-IIID. The Val and Glu at residues 41 and 68 in ω-Aga-IIIA are interchanged in ω-Aga-IIIB, suggesting that these residues are close to each other in the folded protein. The biggest change in sequence between the ω-Aga-IIIAs and the ω-Aga-IIIBs is at residues 49 and 50, where Gln and Gly are replaced by two Arg residues. We speculate that this change is responsible for the differences in potency at L-type Ca channels, but toxin mutagenesis experiments will be necessary to test this idea.

The genetic mechanism for the subtype variants of ω-Aga-IIIA and ω-Aga-IIIB is unknown. The differences among the ω-Aga-IIIB variants, and some of the differences among the major subtypes, could be due to mutations at one of the bases in the triplet codon; Asn and Ser are one base apart in the codon translation table, as are Lys and Arg and the Glu/Val pairings mentioned above. These differences could be due to allelic variation between animals (the starting material is pooled venom from many animals), to variations in RNA splicing or editing, to seasonal variations, or to separate genes. This venom has already been shown to contain many structural variants of a single toxic activity. For example, the Na channel toxins μ-Aga-V and μ-Aga-VI differ from μ-Aga-IV by one and three residues, respectively (Skinner et al., 1989). In fact, we do not believe that we have exhaustively determined

all variants or all members of the type III ω-agatoxin family.

Since *A. aperta* venom contains a large number of homologous ω-agatoxins, one should be concerned with the purity of the toxins that are characterized pharmacologically. We assessed this purity by N-terminal sequencing, by mass spectrometry, and by the degree of separation achieved by HPLC fractionation (see Materials and Methods). We find that contamination of ω-Aga-IIIB or ω-Aga-IIID by ω-Aga-IIIA, which could cause an overestimation of the potency of block of L-type Ca channels, is negligible. In contrast, cross-contamination of the variants of ω-Aga-IIIA or ω-Aga-IIIB could be over 10%, so that we could only detect reliably substantial changes in pharmacological activity. Since we never found potency differences of more than 2-fold among the variants of either toxin, we do not report different values in Table 1.

Studies of Ca currents with locust thoracic neurons reveal that insect neurons have a variety of Ca channel subtypes, some of which are similar to those found in mammalian neurons. Synapses in housefly neuromuscular junctions contain Ca channels that are highly insensitive to ω-Aga-IIIA (Bindokas et al., 1991). Likewise, K^+-induced Ca influx in locust synaptosomes is insensitive to ω-Aga-IIIA (Pocock et al., 1992). In contrast, toxin-sensitive Ca channels are found in locust metathoracic and mesothoracic ganglia neurons (Figure 9). The insensitivity of these Ca channels to ω-CgTx and the block by ω-Aga-IIIA with an IC_{50} of 10–50 nM are similar to the pharmacology of mammalian BI Ca channels (Sather et al., 1993). Since ω-Aga-IIIA and ω-Aga-IIIB are not equipotent at blocking some insect neuronal Ca channels, these toxins might be useful in characterizing variants of mammalian CNS Ca channels.

One of the most important uses for ω-CgTx and the ω-agatoxins is in classifying Ca channels into distinct subtypes. L-, N-, and P-type Ca channels can have very similar gating kinetics, and the distinction among these three channel types is based largely on pharmacological properties. There are two ways to make a pharmacological classification work. The most straightforward, and the one that has generally been used for Ca channels, is to obtain a highly specific drug for each channel type. Thus, the classification scheme for high voltage activated Ca channels presumes that DHPs, ω-CgTx, and ω-Aga-IVA are each specific for a single type of Ca channel. However, as mentioned previously, some of these drugs modify several types of Ca channels, and there are presently more cloned Ca channels than highly specific drugs. An alternative approach has been used for most other receptors for neurotransmitters, where the sequence of relative affinities for a group of drugs is used as a characteristic of a receptor type. It is likely that such a scheme will have to be adopted for voltage-gated Ca channels, as more subtypes of Ca channels are found, as well as new channels that respond to more than one of the "specific" drugs. In such a scheme, ω-Aga-IIIA would be a major element since it blocks L-type and N-type Ca channels with similar high potency, blocks BI Ca channels with 100-fold lower potency, and does not affect T-type Ca channels.

The pharmacology of the type III ω-agatoxins that we report here is based on results obtained with Ca channels expressed in a small sample of tissues, and the above generalizations should be taken as a first approximation. As the toxins are tested against Ca channels in other tissues or cloned channels expressed in functional form, it is likely that the type III ω-agatoxins will exhibit a spectrum of activity on the various isoforms of L-, N-, P-, and possibly T-type Ca channels. For example, we have found that ω-Aga-IIIA blocks L-type Ca channels in guinea pig tracheal smooth muscle about 10-fold less potently than in atria (E.A.E. and C.J.C., unpublished observations). Likewise, there exists electrophysiologically distinct ω-CgTx-sensitive Ca channels, which could also vary in sensitivity to the type III ω-agatoxins. Finally, multiple gene products might actually compose what now appears to be a single pharmacological and/or electrophysiological entity, and these could also be blocked with different potencies by the type III ω-agatoxins. This might explain why the three ω-agatoxins block Ca flux to differing extents (Figure 5).

It has been unclear whether the differences in ω-CgTx sensitivity among types of Ca channels are due to a minor change in the binding site for toxin, such as occurs with isoforms of Na channels that differ in sensitivity to μ-conotoxin. Studies with ω-Aga-IIIA suggest that N- and L-type Ca channels may have similar structures in the mouth of the aqueous pore. Since ω-Aga-IIIA is a potent inhibitor of ω-CgTx binding to rat brain membranes and blocks N- and L-type Ca channels with similar potency, N- and L-type Ca channels might have similar binding sites for ω-Aga-IIIA. This site is most likely located in the mouth of the aqueous pore because the toxin is hydrophilic, does not modify channel gating, and blocks L-type Ca channels in a voltage-independent manner [Mintz et al., 1991; Cohen et al., 1992a; Ertel et al., 1994; but see Mintz (1994)]. In addition, ω-Aga-IIIB recognizes differences between the binding site on the two channels. N- and L-type Ca channels also have a similar subunit composition, $\alpha_1(\alpha_2\delta)\beta$ (Witcher et al., 1993), and the aqueous pore of both channels is formed from the α_1 subunit (Mikami et al., 1989; Perez-Reyes et al., 1989; Williams et al., 1992; Fujita et al., 1993). Thus, the type III ω-agatoxins may be useful for defining the pore geometry of voltage-gated Ca channels.

ACKNOWLEDGMENT

We thank Teresa Bale and Ann Van Dyke for excellent technical assistance, Dr. M. Leibowitz for participation in the early stages of this study and for comments on the manuscript, Keith Elliston for assistance in searching for homologous proteins, and NCBI and the BLAST network service and Drs. J. Calaycay, M.-L. Garcia, G. Kaczorowski, S. Rohrer, C. Rosen, J. Schaeffer, R. Slaughter, A. Smith, and L. Van Der Ploeg for careful reading of versions of the manuscript.

REFERENCES

Adams, B. A., & Beam, K. G. (1989) *J. Gen. Physiol. 94*, 429–444.

Adams, M. E., Herold, E. E., & Venema, V. J. (1989) *J. Comp. Physiol., A 164*, 333–342.

Adams, M. E., Bindokas, V. P., Hasegawa, L., & Venema, V. J. (1990) *J. Biol. Chem. 265*, 861–867.

Almers, W., & McCleskey, E. W. (1984) *J. Physiol. (London) 353*, 585–608.

Artalejo, C. R., Perlman, R. L., & Fox, A. P. (1992) *Neuron 8*, 85–95.

Bean, B. P. (1989) *Annu. Rev. Physiol. 51*, 367–384.

Bindokas, V. P., & Adams, M. E. (1989) *J. Neurobiol. 20*, 171–188.

Bindokas, V. P., Venema, V. J., & Adams, M. E. (1991) *J. Neurophysiol. 66*, 590–601.

Cohen, C. J., Ertel, E. A., Smith, M. M., Venema, V. J., Adams, M. E., & Leibowitz, M. D. (1992a) *Mol. Pharmacol. 42*, 947–951.

Cohen, C. J., Spires, S., & Van Skiver, D. (1992b) *J. Gen. Physiol. 100*, 703–728.

Diniz, C. R., Cordeiro, M. N., Rezende, L. J., Kelly, P., Fischer, S., Reimann, F., Oliveira, E. B., & Richardson, M. (1990) *FEBS Lett. 263*, 251–253.

Ertel, E. A., Cohen, C. J., Leibowitz, M. D., Adams, M., Nguyen, T., Ashley, I. M., & Smith, M. M. (1992) *Biophys. J. 61*, 419a.

Ertel, E. A., Smith, M. M., Leibowitz, M. D., & Cohen, C. J. (1994) *J. Gen. Physiol. 103*, 1–23.

Feigenbaum, P., Garcia, M. L., & Kaczorowski, G. J. (1988) *Biochem. Biophys. Res. Commun. 154*, 298–305.

Forti, L., & Pietrobon, D. (1993) *Neuron 10*, 437–450.

Fujita, Y., Mynlieff, M., Dirksen, R. T., Kim, S.-S., Niidome, T., Nakai, J., Friedrich, T., Iwabe, N., Miyata, T., Furuichi, T., Furutama, D., Mikoshiba, K., Mori, Y., & Beam, K. G. (1993) *Neuron 10*, 585–598.

Hillyard, D. R., Santos, A. D., Monje, V. D., & Adams, M. E. (1994) *Biochemistry* (submitted for publication).

Mikami, A., Imoto, K., Tanabe, T., Niidome, T., Mori, Y., Takeshima, H., Narumiya, S., & Numa, S. (1989) *Nature 340*, 230–233.

Mintz, I. M. (1994) *J. Neurosci.* (in press).

Mintz, I. M., Venema, V. J., Adams, M. E., & Bean, B. P. (1991) *Proc. Natl. Acad. Sci. U.S.A. 88*, 6628–6631.

Mintz, I. M., Adams, M. E., & Bean, B. P. (1992a) *Neuron 9*, 85–95.

Mintz, I. M., Venema, V. J., Swiderek, K. M., Lee, T. D., Bean, B. P., & Adams, M. E. (1992b) *Nature 355*, 827–829.

Mitra, R., & Morad, M. (1985) *Am. J. Physiol. 249*, H1056–H1060.

Perez-Reyes, E., Kim, H. S., Lacerda, A. E., Horne, W., Wei, X., Rampe, D., Campbell, K. P., Brown, A. M., & Birnbaumer, L. (1989) *Nature 340*, 233–236.

Pocock, J. M., Venema, V. J., & Adams, M. E. (1992) *Neurochem. Int. 20*, 263–270.

Sather, W. A., Tanabe, T., Zhang, J.-F., Mori, Y., Adams, M. E., & Tsien, R. W. (1993) *Neuron 11*, 291–303.

Skinner, W. S., Adams, M. E., Quistad, G. B., Kataoka, H., Cesarin, B. J., Enderlin, F. E., & Schooley, D. A. (1989) *J. Biol. Chem. 264*, 2150–2155.

Snutch, T. P., & Reiner, P. B. (1992) *Curr. Opin. Neurobiol. 2*, 247–253.

Soong, T. W., Stea, A., Hodson, C. D., Dubel, S. J., Vincent, S. R., & Snutch, T. P. (1993) *Science 260*, 1133–1136.

Suter, C., & Usherwood, P. N. R. (1985) *Comp. Biochem. Physiol. 80C*, 221–229.

Tsien, R. W., Ellinor, P. T., & Horne, W. A. (1991) *Trends Pharmacol. Sci. 12*, 349–354.

Turner, T. J., Adams, M. E., & Dunlap, K. (1992) *Science 258*, 310–313.

Turner, T. J., Adams, M. E., & Dunlap, K. (1993) *Proc. Natl. Acad. Sci. U.S.A. 90*, 9518–9522.

Venema, V. J., Swiderek, K. M., Lee, T. D., Hathaway, G. M., & Adams, M. E. (1992) *J. Biol. Chem. 267*, 2610–2615.

Wang, X., Treistman, S. N., & Lemos, J. R. (1992) *J. Physiol. (London) 445*, 181–199.

Williams, M. E., Brust, P. F., Feldman, D. H., Patthi, S., Simerson, S., Maroufi, S., McCue, A. F., Velicelebi, G., Ellis, S. B., & Harpold, M. M. (1992) *Science 257*, 389–395.

Witcher, D. R., De Waard, M., Sakamoto, J., Franzini-Armstrong, C., Pragnell, M., Kahl, S. D., & Campbell, K. P. (1993) *Science 261*, 486–489.